Chemical and Magnetic Inequivalence of Glycerol Protons in Individual Subclasses of Choline Glycerophospholipids: Implications for Subclass-Specific Changes in Membrane Conformational States

Xianlin Han,[†,‡] Xi Chen,[†] and Richard W. Gross*[,†,‡]

Contribution from the Departments of Chemistry and Medicine, Washington University, St. Louis, Missouri 63110. *Received April 1, 1991*

Abstract: High-resolution ^1H NMR spectroscopy and subsequent computer simulations of experimental spectra of multiple molecular species in each choline glycerophospholipid subclass demonstrated that (1) the two diastereotopic sn-3 methylene protons of the glycerol backbone in ether-linked phospholipids are more chemically and magnetically inequivalent than comparable protons present in conventionally studied phosphatidylcholine (e.g., $\Delta\delta$ = 0, 0.02, and 0.04 ppm for phosphatidylcholine, plasmenylcholine, and plasmanylcholine, respectively); (2) the two diastereotopic sn-1 methylene protons of the glycerol backbone in ether-linked phospholipids are more chemically and magnetically equivalent than their counterparts in phosphatidylcholine (e.g., $\Delta\delta$ = 0.26, 0.07, and 0.04 ppm and $^2J_{HH}$ = 12.0, 11.5, and 10.8 Hz for phosphatidylcholine, plasmenylcholine, and plasmanylcholine, respectively); (3) the sn-2 methine proton is more shielded in ether-linked glycerophospholipids in comparisons to diacyl phospholipids; and (4) the vicinal spin coupling constants of protons in the glycerol backbone are distinct in each subclass. Analysis of this data utilizing a three staggered state conformational model demonstrated that modest alterations in the molecular geometry of the proximal portion of the sn-1 aliphatic chain in each choline glycerophospholipid subclass result in changes in the distribution of the conformational states of the glycerol backbone. Such alterations in the distribution of conformational states at the aqueous interface may be important determinants of the specific functional characteristics of subcellular membranes enriched in ether-linked phospholipids.

Introduction

Definitive correlation of the relationship of phospholipid chemical structure to biologic membrane function has been a long-standing objective of modern membrane chemistry. Alterations in the relative distribution of the conformational states assumed by the glycerol backbone are accompanied by critical changes in the time-averaged stereoelectronic relationships in the proximal portions of each aliphatic chain that collectively contribute to the physical and dynamic properties of phospholipid aggregates. Thus, the role of the glycerol backbone as a primary determinant of the distribution of conformational states in mammalian membranes has long been recognized.[1-3] Recently, Hauser et al.[4] demonstrated that the preferred conformation of the glycerol backbone in phosphatidylcholine is independent of the length of the acyl chain and that similar distributions of conformational states are present in either the micellar or bilayer aggregation states. Furthermore, analyses of ^2H NMR line shape and spin-lattice relaxation time behavior have demonstrated that the motion in the glycerol backbone is best described (to a first approximation) by an internal jump model with motion along the sn-1-sn-2 glycerol C-C bond in both diacyl glycolipid and diacyl phospholipid bilayers.[5]

Although the overwhelming majority of physical studies on naturally occurring phospholipids have examined the molecular dynamics and conformation of diacyl phospholipid molecular species, some subcellular membranes contain a predominance of plasmalogen molecular species.[6,7] The molecular dynamics of plasmalogen and diacyl phospholipid molecular species are distinct in both the membrane interior and near the hydrophobic/hydrophilic interface.[8,9] Furthermore, conformational analysis of the proximal region of the aliphatic chains in plasmenylcholine bilayers by truncated driven nuclear Overhauser enhancement has demonstrated that the presence of the vinyl ether linkage in plasmalogen molecular species results in substantial changes in the molecular geometry of the proximal portion of the sn-2 chain[10] from that initially ascertained from crystallographic studies of phosphatidylcholine[11] and subsequently confirmed by solution-state ^2H NMR spectroscopy.[12] To directly compare the conformational states of the glycerol backbone in each of the three major subclasses of mammalian choline glycerophospholipids, we determined critical geminal and vicinal ^1H-^1H as well as ^1H-^{31}P coupling constants through computer simulations of experimental 500-MHz ^1H high-resolution NMR spectra utilizing multiple molecular species of phosphatidylcholine, plasmenylcholine, and plasmanylcholine. We now report that the sn-1 and sn-3 protons of the glycerol backbone in each of the subclasses of choline glycerophospholipids are chemically and magnetically inequivalent and that distinct vicinal ^1H-^1H and ^1H-^{31}P spin coupling constants are present. Collectively, these results demonstrate that covalent modification of the proximal portion of the sn-1 aliphatic chain results in substantial and differential effects on the molecular conformation of the glycerol backbone in each choline glycerophospholipid subclass.

Experimental Section

Materials. 1,2-Dihexadecanoyl-*sn*-glycero-3-phosphocholine (PP phosphatidylcholine), 1-hexadecanoyl-2-eicosa-5′,8′,11′,14′-tetraenoyl-*sn*-glycero-3-phosphocholine (PA phosphatidylcholine), 1-hexadecanoyl-2-octadec-9′-enoyl-*sn*-glycero-3-phosphocholine (PO phosphatidylcholine), bovine heart lecithin, and a mixture of 1-*O*-alkyl-*sn*-glycero-3-phosphocholines (predominantly 16:0 and 18:0 alkyl ethers) (lyso-PAF) were purchased from Avanti Polar Lipids, Inc. (Alabaster, AL). Arachidonoyl chloride, oleoyl chloride, and palmitoyl chloride were obtained from Nu Chek Prep, Inc. (Elysian, MN). *N*,*N*-Dimethyl-4-aminopyridine was obtained from Aldrich Chemical Co. (Milwaukee, WI).

* To whom correspondence should be addressed at the Washington University School of Medicine, 660 South Euclid Avenue, Box 8020, St. Louis, MO 63110.
† Department of Chemistry.
‡ Department of Medicine.

(1) Seelig, J. *Q. Rev. Biophys.* **1977**, *10*, 353-418.
(2) Seelig, J.; Seelig, A. *Q. Rev. Biophys.* **1980**, *13*, 19-61.
(3) Hauser, H.; Pascher, I.; Pearson, R. H.; Sundell, S. *Biochim. Biophys. Acta* **1981**, *650*, 21-51.
(4) Hauser, H.; Pascher, I.; Sundell, S. *Biochemistry* **1988**, *27*, 9166-9174.
(5) Auger, M.; van Calsteren, M.; Smith, I. C. P.; Jarrell, H. C. *Biochemistry* **1990**, *29*, 5815-5821.
(6) Gross, R. W. *Biochemistry* **1984**, *23*, 158-165.
(7) Gross, R. W. *Biochemistry* **1985**, *24*, 1662-1668.
(8) Pak, J. H.; Bork, V. P.; Norberg, R. E.; Creer, M. H.; Wolf, R. A.; Gross, R. W. *Biochemistry* **1987**, *26*, 4824-4830.
(9) Han, X.; Gross, R. W. *Biochim. Biophys. Acta* **1991**, *1063*, 129-136.
(10) Han, X.; Gross, R. W. *Biochemistry* **1990**, *29*, 4992-4996.
(11) Pearson, R. H.; Pascher, I. *Nature* **1979**, *281*, 499-501.
(12) Seelig, J.; Browning, J. L. *FEBS Lett.* **1978**, *92*, 41-44.

0002-7863/91/1513-7104$02.50/0

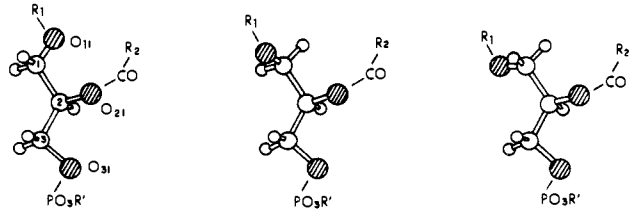

Figure 1. The three minimum free energy staggered conformational states of the glycerol C_1–C_2 bond in glycerophospholipids. Rotamers a–c are defined by alterations in the two related torsion angles, $\theta_1 = O_{11}$–C_1–C_2–C_3 and $\theta_2 = O_{11}$–C_1–C_2–O_{21}. The torsion angle θ_2 in rotamers a and b corresponds to the ±-synclinal (i.e., ±-gauche) conformation of the C_1–C_2 bond in the glycerol backbone while θ_2 in rotamer c represents the antiperiplanar conformation of the C_1–C_2 bond in the glycerol backbone. R_1 at the sn-1 aliphatic chain is linked by ester, vinyl ether, or alkyl ether substituents corresponding to each of the three subclasses of glycerophospholipids shown in Figure 2. R_2 represents the aliphatic ester-linked substituent at the sn-2 carbon. R′ represents the base covalently attached to the glycerol backbone through a phosphodiester linkage. The standard IUPAC nomenclature is used.

Homogeneous 1-*O*-(*Z*)-hexadec-1′-enyl-*sn*-glycero-3-phosphocholine (lysoplasmenylcholine) was prepared from bovine heart lecithin as previously described.[13] Homogeneous 1-*O*-(*Z*)-hexadec-1′-enyl-2-eicosa-5′,8′,11′,14′-tetraenoyl-*sn*-glycero-3-phosphocholine (PA plasmenylcholine), 1-*O*-(*Z*)-hexadec-1′-enyl-2-hexadecanoyl-*sn*-glycero-3-phosphocholine (PP plasmenylcholine), and 1-*O*-(*Z*)-hexadec-1′-enyl-2-octadec-9′-enoyl-*sn*-glycero-3-phosphocholine (PO plasmenylcholine) were synthesized by *N*,*N*-dimethyl-4-aminopyridine-catalyzed condensation of the corresponding acyl chloride with lysoplasmenylcholine and purified by straight-phase HPLC as previously described.[9,14] 1-*O*-Alkyl-2-eicosa-5′,8′,11′,14′-tetraenoyl-*sn*-glycero-3-phosphocholine, 1-*O*-alkyl-2-octadec-9′-enoyl-*sn*-glycero-3-phosphocholine, and 1-*O*-alkyl-2-hexadecanoyl-*sn*-glycero-3-phosphocholine were synthesized similarly by *N*,*N*-dimethyl-4-aminopyridine-catalyzed condensation of the corresponding acyl chloride with 1-*O*-alkyl-*sn*-glycero-3-phosphocholine and purified by straight-phase HPLC.[14] Homogeneous 1-*O*-hexadecyl-2-eicosa-5′,8′,11′,14′-tetraenoyl-*sn*-glycero-3-phosphocholine (PA plasmanylcholine), 1-*O*-hexadecyl-2-octadec-9′-enoyl-*sn*-glycero-3-phosphocholine (PO plasmanylcholine), and 1-*O*-hexadecyl-2-hexadecanoyl-*sn*-glycero-3-phosphocholine (PP plasmanylcholine) were separated by isocratic reverse-phase HPLC utilizing an Ultrasphere octadecyl silica column (10 × 250 mm; 5 μm particles (Beckman, CA)) employing a mobile phase of 90.5:7:2.5 methanol/water/acetonitrile (v/v/v) containing 20 mM choline chloride. All phospholipids were characterized by TLC, ^{1}H NMR, and fast atom bombardment mass spectroscopy and quantified by capillary gas–liquid chromatography after acid methanolysis.[6,14,15]

Preparation of NMR Samples. Homogeneous phospholipids in chloroform stock solution were initially dried under a nitrogen stream prior to exhaustive evacuation (50 mTorr) for a minimum of 4 h. An appropriate volume of $CDCl_3$–CD_3OD (2:1, v/v) and 0.01% tetramethylsilane were added to the dried choline glycerophospholipids to yield a 30 mM final concentration of lipid. The sample was vortexed, and the resultant phospholipid micelles[4,16] were directly analyzed by NMR spectroscopy.

NMR Spectroscopy. High-resolution ^{1}H NMR spectra of phospholipids were obtained by utilizing a Varian VXR-500 spectrometer operating at 500 MHz with a digital resolution of 0.18 Hz/point. All experiments were performed at 25.0 ± 0.5 °C. The chemical shifts and coupling constants of the resonances from the protons in the glycerol backbone of all phospholipids were obtained from computer simulations of experimental spectra utilizing the program LAOCOON[17] with magnetic equivalence added on a SUN-4 host computer equipped with a 150-Mbyte disk memory. The accuracy of spin coupling constants derived from the spectral simulation was 0.05–0.1 Hz. The fractional populations of the major conformational rotamers were calculated from the observed vicinal spin coupling constants on the basis of the assumption that the observed coupling constants represented averages of the component coupling constants of each of the three staggered conformers (e.g., rotamers a–c in Figure 1), which are weighted by their fractional populations.[18-20] Utilizing a generalized Karplus equation,[21,22] we found that alterations in the electronegativity and orientation of the proximal portion of the sn-1 aliphatic chain in the three subclasses of choline glycerophospholipids result in only diminutive changes in the vincinal spin coupling constants. The error in the calculated fractional populations was less than 5% as ascertained from the error of vicinal spin–spin coupling constants calculated by analysis of error propagation.

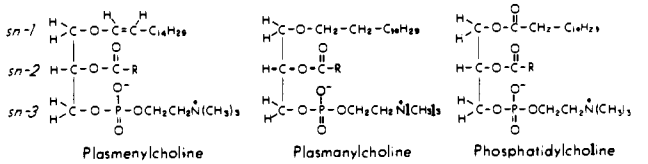

Figure 2. Molecular structures of the choline glycerophospholipid subclasses. The aliphatic chain R = $C_{15}H_{31}$, $C_{17}H_{33}$, or $C_{19}H_{31}$ corresponds to palmitic, oleic, or arachidonic acid at the sn-2 position in the glycerol backbone, respectively.

Results

Each of the six major naturally abundant molecular species of vinyl ether and alkyl ether choline glycerophospholipids (Figure 2) were synthesized and subsequently purified by sequential straight- and reverse-phase HPLC prior to conformational analyses of the glycerol backbone by 500-MHz ^{1}H high-resolution NMR spectroscopy. Assignments of individual protons of the glycerol backbone in both synthetic ether-linked choline glycerophospholipids and commercially available diacyl choline glycerophospholipids were made by utilizing homo- and heteronuclear (e.g., ^{1}H–^{31}P) double-resonance experiments. High-resolution ^{1}H NMR spectra of plasmenylcholines were distinguished by the presence of the anticipated resonances at 4.37 and 5.94 ppm corresponding to the β- and α-vinyl ether protons (e.g., Figure 3, top). Similarly, ^{1}H NMR spectra of plasmanylcholines contained a peak at 3.45 ppm corresponding to the O–CH_2 resonance at the sn-1 position (e.g., Figure 3, middle). Finally, spectra of PP phosphatidylcholine were indistinguishable from previously published high-resolution NMR spectra.[19]

As is evident from experimental spectra, the proton resonances in the glycerol backbone of PP plasmenylcholine and PP plasmanylcholine differed substantially (compare Figure 4A,B). Furthermore, both were markedly different from the previously characterized resonances of protons in the glycerol backbone in PP phosphatidylcholine (Figure 4C). Since the conformation of the glycerol backbone is a primary determinant of the spatial relationship of the aliphatic chains in each lipid subclass, spectral simulations of experimental spectra of protons in the glycerol backbone in each molecular species and molecular subclass were performed. The chemical shifts as well as the geminal and vicinal spin coupling constants of protons in the glycerol backbone (from analyses of computer simulations of experimental spectra as described in the Experimental Section) are listed in Table I. The results demonstrate that the chemical shifts of the sn-1 methylene protons in the glycerol backbone are altered by the nature of the covalent linkage in each subclass of choline glycerophospholipids (Table I). The experimentally and computationally determined values of the chemical shifts and coupling constants of protons in disaturated PP phosphatidylcholine are in excellent agreement with previously published studies.[4,19] Surprisingly, the chemical shift differences between each diastereotopic proton in the sn-1 position of the glycerol backbone are largest for each molecular species of phosphatidylcholine in multiple comparisons to corresponding molecular species of the sn-1 protons in vinyl ether or

(13) Wolf, R. A.; Gross, R. W. *J. Lipid Res.* **1985**, *26*, 629–633.
(14) Han, X. Ph.D. Thesis, Washington University, St. Louis, MO, 1990.
(15) Fink, K. L.; Gross, R. W. *Circ. Res.* **1984**, *55*, 585–594.
(16) Derivichian, O. C. *Prog. Biophys. Mol. Biol.* **1964**, *14*, 263–342.
(17) Swalen, J. D. *Progress in NMR Spectroscopy*; Pergamon Press: Oxford, 1966; Vol. 1, Chapter 3, pp 205–250.
(18) Hauser, H.; Guyer, W.; Levine, B.; Skrabal, P.; Williams, R. J. *Biochim. Biophys. Acta* **1978**, *508*, 450–463.
(19) Hauser, H.; Guyer, W.; Pascher, I.; Skrabal, P.; Sundell, S. *Biochemistry* **1980**, *19*, 366–373.
(20) Hauser, H.; Guyer, W.; Spiess, M.; Pascher, I.; Sundell, S. *J. Mol. Biol.* **1980**, *137*, 265–282.
(21) Haasnoot, C. A. G.; de Leeuw, F. A. A. M.; Altona, C. *Tetrahedron* **1980**, *36*, 2783–2792.
(22) Colucci, W. J.; Jungk, S. J.; Gandour, R. D. *Magn. Reson. Chem.* **1985**, *23*, 335–343.

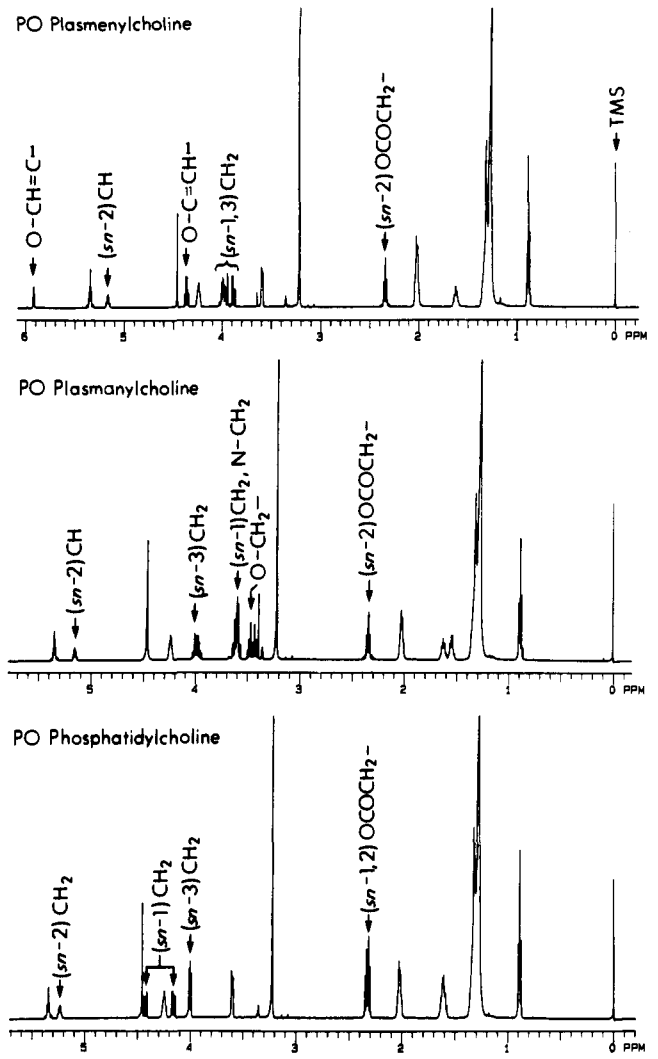

Figure 3. 500-MHz ^1H NMR spectra of the three subclasses of choline glycerophospholipids. The NMR spectrum (top) of 1-*O*-(*Z*)-hexadec-1′-enyl-2-octadec-9′-enoyl-*sn*-glycero-3-phosphocholine (PO plasmenylcholine) is distinguished by the presence of resonances corresponding to the α- and β-vinyl ether protons at 5.94 and 4.37 ppm, respectively. The spectrum (middle) of 1-*O*-hexadecyl-2-octadec-9′-enoyl-*sn*-glycero-3-phosphocholine (PO plasmanylcholine) is distinguished by the resonance at 3.45 ppm corresponding to the sn-1 ether-linked methylene protons ($-O-CH_2-$). The spectrum (bottom) of 1-hexadecanoyl-2-octadec-9′-enoyl-*sn*-glycero-3-phosphocholine (PO phosphatidylcholine) is distinguished by a comparatively high intensity of the $OCOCH_2$ resonance (2.34 ppm) resulting from acyl groups at both the sn-1 and sn-2 positions. All chemical shifts are referenced to the internal standard tetramethylsilane. All spectra were obtained by utilizing 30 mM of each choline glycerophospholipid in $CDCl_3$–CD_3OD (2:1, v/v) as described in the Experimental Section.

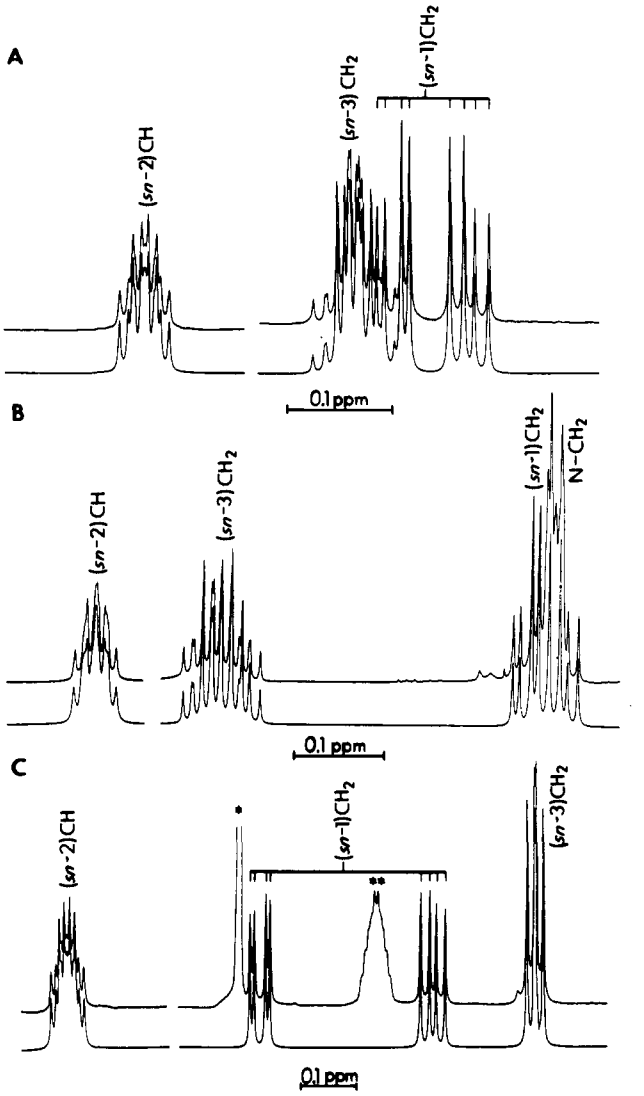

Figure 4. Expanded spectra and computer simulations of the glycerol protons in choline glycerophospholipid subclasses containing palmitic acid at the sn-2 position. (A) The experimental NMR spectrum corresponding to glycerol protons (top) and the corresponding computer simulation (bottom) of 1-*O*-(*Z*)-hexadec-1′-enyl-2-hexadecanoyl-*sn*-glycero-3-phosphocholine (PP plasmenylcholine) in $CDCl_3$–CD_3OD (2:1, v/v) at 25 °C. (B) The experimental NMR spectrum corresponding to glycerol protons (top) and the corresponding computer simulation (bottom) of 1-*O*-hexadecyl-2-hexadecanoyl-*sn*-glycero-3-phosphocholine (PP plasmanylcholine) in $CDCl_3$–CD_3OD (2:1, v/v) at 25 °C. Because the glycerol sn-1 methylene resonance in plasmanylcholine partially overlaps with its α-choline methylene ($N-CH_2$) resonance, these assignments were made by homonuclear double-resonance experiments on the β-choline methylene protons ($N-C-CH_2$), which simplified the α-choline methylene proton resonance. (C) The experimental NMR spectrum corresponding to the glycerol protons (top) and the corresponding computer simulation (bottom) of 1,2-dihexadecanoyl-*sn*-glycero-3-phosphocholine (PP phosphatidylcholine) in $CDCl_3$–CD_3OD (2:1, v/v) at 25 °C. The peaks marked with * and ** are CD_3OH (solvent) and $N-C-CH_2$ (β-choline methylene) resonances, respectively. The distinct individual chemical shifts of each of the protons in the glycerol backbone are shown in Figure 3 and Table I.

alkyl ether choline glycerophospholipids (e.g., $\Delta\delta$ = 0.26 ppm in each phosphatidylcholine, 0.07 ppm in each plasmenylcholine, and 0.04 ppm in each plasmanylcholine between the sn-1 diastereotopic protons (Table I)). Similarly, the spin coupling constants between the two diastereotopic sn-1 methylene protons of the glycerol backbone are smaller in ether-linked phospholipids in comparison to their ester-linked phospholipid counterparts (e.g., 12.0 Hz for phosphatidylcholines, 11.5 Hz for plasmenylcholines, and 10.8 Hz for plasmanylcholines (Table I)). Thus, the sn-1 glycerol methylene protons in all three subclasses give rise to an octet spectrum characteristic of an ABX spin system (Figure 4A–C), demonstrating that the two sn-1 methylene protons of the glycerol backbone are both chemically and magnetically inequivalent. The magnitude of inequivalence in ether-linked phospholipids is smaller than that present in previously analyzed ester-linked phospholipid species, suggesting that each proton in ether-linked phospholipids is more symmetrically oriented toward the sn-2 ester and/or the sn-3 phosphodiester linkages in the glycerol backbone.

The sn-3 methylene protons in the glycerol backbone were identified by irradiation of either the ^{31}P resonance or the sn-2 methine proton. Although the sn-3 methylene protons in each molecular species of phosphatidylcholine resulted in a quartet spectrum, corresponding protons in each subclass of ether-linked phospholipids (plasmenylcholine and plasmanylcholine) gave rise to a complex multiplet resulting from the chemical and magnetic inequivalence of each sn-3 diastereotopic proton (Figure 4). Specifically, although each diastereotopic proton in the sn-3

Table I. Chemical Shifts and Coupling Constants of Glycerol Protons in the Three Subclasses of Choline Glycerophospholipids[a]

molecular species	chemical shift (ppm)[b]					coupling constant (Hz)[c]							
	A[d]	B	C	D	E	J_{AB}	J_{AC}	J_{BC}	J_{DE}	J_{CD}	J_{CE}	J_{DP}	J_{EP}
PP phosphatidylcholine	4.167	4.428	5.238	4.008	4.008	12.04	7.04	3.21	[e]	5.51	5.57	6.94	6.89
PO phosphatidylcholine	4.164	4.428	5.239	4.007	4.006	12.00	6.97	3.18		5.61	5.62	6.95	6.84
PA phosphatidylcholine	4.164	4.429	5.241	4.009	4.008	12.01	6.90	3.23		5.48	5.54	6.98	6.89
PP plasmenylcholine	3.887	3.954	5.171	4.002	3.982	11.52	6.66	3.60	11.01	5.40	5.54	6.18	6.86
PO plasmenylcholine	3.886	3.954	5.171	4.002	3.982	11.51	6.66	3.58	10.99	5.37	5.57	6.15	6.86
PA plasmenylcholine	3.887	3.955	5.176	4.010	3.986	11.50	6.59	3.68	11.02	5.31	5.44	6.31	6.71
PP plasmanylcholine	3.587	3.626	5.153	4.006	3.967	10.86	6.45	3.84	11.00	4.82	6.62	6.12	6.19
PO plasmanylcholine	3.587	3.626	5.154	4.006	3.967	10.87	6.45	3.85	11.00	4.83	6.64	6.11	6.20
PA plasmanylcholine	3.585	3.624	5.158	4.011	3.969	10.77	6.45	3.81	11.11	4.89	6.72	6.18	6.24

[a] All experiments were performed in $CDCl_3$–CD_3OD (2:1, v/v) at 25 °C on a Varian VXR-500. [b] Chemical shifts are expressed in parts per million downfield from tetramethylsilane. The accuracy of the chemical shifts is ±0.001 ppm. [c] Coupling constants were obtained from computer simulations of experimental spectra. The accuracy of the coupling constants is 0.05–0.1 Hz. [d] Protons in the glycerol backbone are labeled as follows:

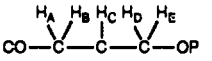

[e] Due to the equivalence of the CH_2 protons in phosphatidylcholine, the geminal coupling constants in this subclass are not observed.

position in the glycerol backbone of phosphatidylcholine had identical chemical shifts, the two diastereotopic protons present at the sn-3 position in plasmenylcholine and plasmanylcholine differed by 0.02 and 0.04 ppm, respectively (Table I). Calculation of the coupling constants from spectral simulations demonstrated that the coupling of both sn-3 methylene protons with the sn-2 methine proton was similar in each molecular species of phosphatidylcholine and plasmenylcholine, but was substantially different in plasmanylcholine (Table I). The couplings between the sn-3 methylene protons in plasmanylcholines and the phosphorous atom were similar for each diastereotopic proton but differed substantially in magnitude compared to their phosphatidylcholine counterparts (Table I). The couplings between the sn-3 methylene protons in plasmenylcholine and the phosphorous atom were different for each diastereotopic sn-3 methylene proton and were characterized by coupling constants that were similar to those of phosphatidylcholine for one proton and similar to those for plasmanylcholine for the other proton (Table I).

The sn-2 methine proton of the glycerol backbone in each choline glycerophospholipid subclass possessed distinct chemical shifts. These differences in the chemical shifts were reproducibly present in each molecular species of each of the three choline glycerophospholipid subclasses examined (Table I). Thus, modification of the nature of the covalent linkage at the proximal portion of the sn-1 position alters the chemical environment of the sn-2 methine proton.

To examine the influence of the nature of the sn-2 aliphatic constituent (i.e., chain length, position, and degree of unsaturation) in individual molecular species of each choline glycerophospholipid subclass, comparisons of the chemical shifts and coupling constants of glycerol protons in nine individual molecular species were made. The chemical shifts and coupling constants of each glycerol backbone proton in phosphatidylcholine, plasmenylcholine, and plasmanylcholine containing palmitic acid at the sn-2 position did not differ (within experimental error) from corresponding lipids in each subclass containing oleic acid at the sn-2 position (Table I). High-resolution spectra of phosphatidylcholine, plasmenylcholine, and plasmanylcholine subclasses containing arachidonic acid at the sn-2 position demonstrated only modest differences compared to identical choline glycerophospholipid subclasses containing palmitic or oleic acid at the sn-2 position. The changes induced by arachidonic acid were small in comparison to the differences induced by alterations in the proximal portion of the sn-1 aliphatic chain in each subclass (Table I, Figure 5A–C). Thus, alterations in choline glycerophospholipid subclasses have substantially larger effects on the distribution of conformational states of the glyercol backbone than do alterations in the nature of the fatty acyl substituent at the sn-2 position in these systems.

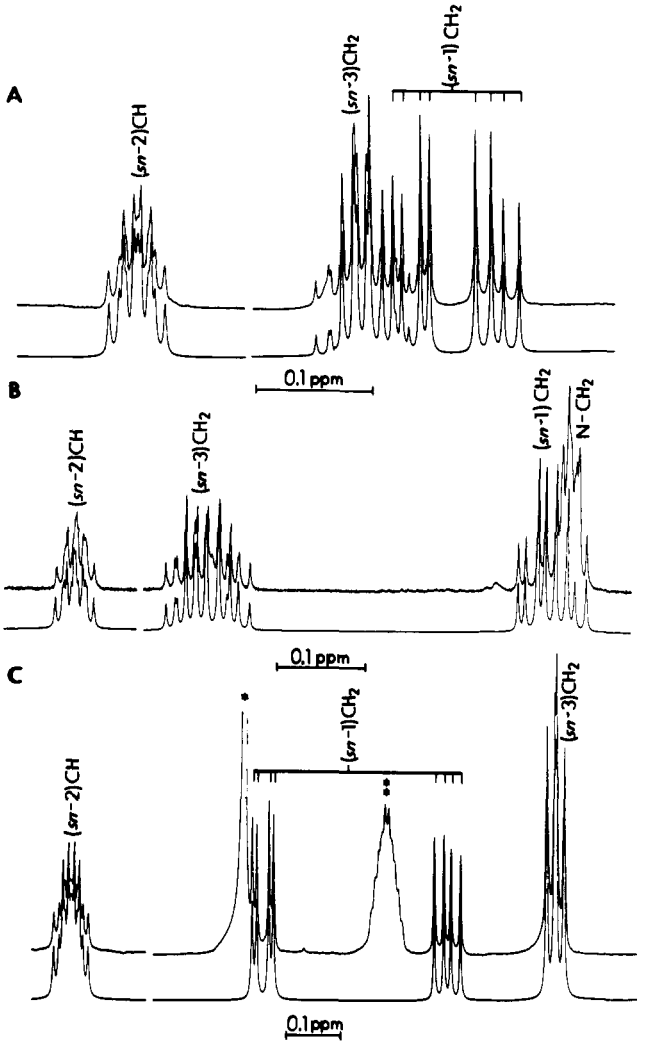

Figure 5. Expanded spectra and computer stimulations of the glycerol protons in choline glycerophospholipids containting arachiodonic acid at the sn-2 position. Expanded expectra (top) and computer simulations (bottom) of the glycerol protons in (A) PA plasmenylcholine, (B) PA plasmanylcholine, and (C) PA phosphatidylcholine were obtained as described in the caption to Figure 4.

Discussion

The results of the present study are the first to demonstrate the chemical and magnetic inequivalance of protons in the glycerol backbone in each molecular subclass of choline glycerophospholipids. Specifically, computer simulations of experimental NMR spectra demonstrate that (1) the two diastereotopic sn-3 methylene protons of the glycerol backbone in ether-linked phospholipids are more chemically and magnetically inequivalent than comparable protons present in conventionally studied phosphatidylcholine; (2)

Table II. Staggered-State Rotameric Distributions of Minimum Energy Conformations in the Glycerol Backbone of Choline Glycerophospholipid Subclasses[a]

molecular species	θ_1/θ_2[b] a	b	c	$\gamma_1(C_2-C_3-O_{31}-P)$ ±-gauche	antiperiplanar
PP phosphatidylcholine	51.8 ± 1.8 (1.3 ± 0.1)	39.7 ± 1.2 (49.9 ± 1.4)	8.5 ± 0.3 (48.8 ± 1.4)	31.1 ± 1.3	68.9 ± 2.5
PO phosphatidylcholine	51.4 ± 1.7 (1.3 ± 0.1)	40.4 ± 1.2 (50.6 ± 1.5)	8.2 ± 0.3 (48.1 ± 1.4)	30.9 ± 1.2	69.1 ± 2.5
PA phosphatidylcholine	50.5 ± 1.5 (2.0 ± 0.1)	40.8 ± 1.3 (50.6 ± 1.5)	8.7 ± 0.3 (47.4 ± 1.3)	31.4 ± 1.3	68.6 ± 2.5
PP plasmenylcholine	46.7 ± 1.2 (6.4 ± 0.2)	40.7 ± 1.2 (48.8 ± 1.4)	12.6 ± 0.4 (44.8 ± 1.4)	26.0 ± 1.0	74.0 ± 2.8
PO plasmenylcholine	46.8 ± 1.2 (6.2 ± 0.2)	40.8 ± 1.2 (49.0 ± 1.4)	12.4 ± 0.4 (44.8 ± 1.4)	25.9 ± 1.0	74.1 ± 2.8
PA plasmenylcholine	45.7 ± 1.1 (7.3 ± 0.2)	40.8 ± 1.2 (48.6 ± 1.4)	13.5 ± 0.4 (44.1 ± 1.4)	25.9 ± 1.0	74.1 ± 2.8
PP plasmanylcholine	43.7 ± 1.1 (9.4 ± 0.3)	41.1 ± 1.2 (48.0 ± 1.4)	15.2 ± 0.5 (42.6 ± 1.3)	21.3 ± 0.8	78.7 ± 3.0
PO plasmanylcholine	43.7 ± 1.1 (9.4 ± 0.3)	41.0 ± 1.2 (48.0 ± 1.4)	15.3 ± 0.5 (42.6 ± 1.3)	21.3 ± 0.8	78.7 ± 3.0
PA plasmanylcholine	44.0 ± 1.1 (9.1 ± 0.3)	41.2 ± 1.2 (48.3 ± 1.4)	14.8 ± 0.5 (42.6 ± 1.3)	22.0 ± 0.8	78.0 ± 3.0

[a] Rotameric distributions were calculated from the observed vicinal spin coupling constants in Table I as described in the Experimental Section and are expressed in percentages. [b] For torsion angles θ_1 and θ_2 (refer to Figure 1), the rotameric distributions have been calculated by utilizing $J_{AC} > J_{BC}$ or $J_{AC} < J_{BC}$ (values in parentheses). Rotamers a–c are shown in Figure 1.

the two sn-1 methylene protons of the glycerol backbone in ether-linked phospholipids are more chemically and magnetically equivalent than their counterparts in phosphatidylcholine; (3) the sn-2 methine proton is more shielded in ether-linked glycerophospholipids in comparisons with conventional diacyl phospholipids; and (4) the vicinal spin coupling constants of protons in the glycerol backbone are distinct in each subclass.

When the frequently employed assumption that the majority of relevant conformational states can be described by a three staggered state conformational model representing minimum free energy conformations is utilized, additional insights into differences in the conformational states of ether-linked and diacyl choline glycerophospholipids can be made. In this model, the vicinal spin coupling constants in each of the three possible conformations can be utilized as component coupling constants[4,18,20] to determine the time-averaged distribution of major conformational states from published values of component coupling constants.[4,23,24] Since experimental spectra were successfully simulated by utilizing only one set of vicinal spin coupling constants for each C–C or C–O bond, motional averaging between each of the three staggered conformations must occur that is fast on the NMR time scale. The fractional populations of rotamers a–c about the glycerol C_1–C_2 bond (Figure 1) were calculated and are summarized in Table II. Initially, we have allowed $J_{AC} > J_{BC}$ as has been conventionally assumed in analyses of phosphatidylcholines where parallel alignment of the two aliphatic chains precludes antiperiplanar rotamer c (Figure 1) as the major conformational state.[4,19] By conventional assignment (i.e., $J_{AC} > J_{BC}$), the population of the rotamer c is present in the rank order plasmanylcholine > plasmenylcholine > phosphatidylcholine. We note that the population of the antiperiplanar rotamer c (again assuming $J_{AC} > J_{BC}$) in plasmanylcholine is almost twice that present in phosphatidylcholine. However, it is important to note that both plasmanylcholine and plasmenylcholine are not subject to the same types of conformational constraints as those imposed on phosphatidylcholine by virtue of their disparate molecular geometries in the proximal portion of the sn-1 aliphatic chain. Specifically, the antiperiplanar conformation of the sn-1 and sn-2 oxygen atoms (i.e., O_{11} and O_{21}) in plasmenylcholine and plasmanylcholine (rotamer c) is entirely compatible with a compact arrangement of both the sn-1 and sn-2 aliphatic chains. This results largely from the fact that the antiperiplanar conformation (rotamer c) in phosphatidylcholine requires that the sn-1 carbonyl is directed into the hydrophobic portion of the membrane (assuming a trans conformation of the sn-1 ester), which seems unlikely on the basis of energetic considerations and is not present in the crystal structure of phosphatidylcholine. However, the geometry of the vinyl ether constituent is precisely tailored to adopt an antiperiplanar conformation in which the aliphatic chains are in close spatial proximity. Analyses of monomeric plasmenylcholine and phosphatidylcholine utilizing MM2-based calculations demonstrate that plasmenylcholine, but not phosphatidylcholine, can efficiently pack in a pseudo-antiperiplanar conformation (i.e., $\theta_2 = 130°$) (Figure 6). We note that the proposed conformation of the vinyl ether linkage in rotamer c is strikingly similar to the minimal energy conformation of the vinyl ether linkage in methyl vinyl ether as determined by utilizing MM2 calculations.[25] Support for this conformation of the glycerol backbone in plasmenylcholine has recently been obtained by utilizing truncated driven nuclear Overhauser enhancement NMR.[10] Accordingly, the possibility that $J_{BC} > J_{AC}$ in both plasmenylcholine and plasmanylcholine cannot be excluded on the basis of steric constraints alone. Calculation of the relative distribution of conformational states utilizing $J_{BC} > J_{AC}$ demonstrates that rotamers b and c are the two predominant conformational states for ether-linked glycerophospholipids in this paradigm (Table II). Whatever the case (i.e., $J_{AC} > J_{BC}$ or $J_{BC} > J_{AC}$), these results demonstrate that the statistical distribution of rotamer c is substantially different in

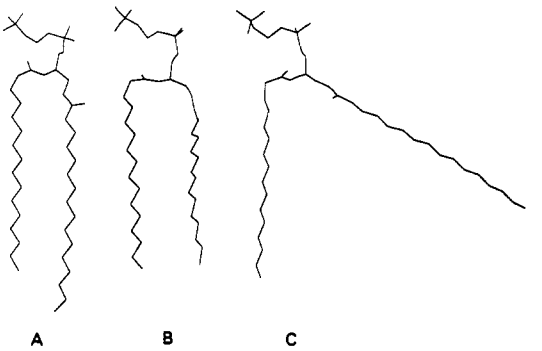

Figure 6. Energy-minimized conformations of monomeric phosphatidylcholine and plasmenylcholine. (A) Coordinates from the crystal structure of phosphatidylethanolamine[30] were utilized as the basis set for MM2 calculations of the minimum energy conformation of PP phosphatidylcholine. (B) The torsion angle θ_2 (O_{11}–C_1–C_2-O_{21}) in the glycerol backbone in plasmenylcholine was arranged in a pseudo-antiperiplanar conformation ($\theta_2 = 130°$), and the remaining crystal structure coordinates of phosphatidylethanolamine[30] were utilized as the basis set for energy minimization utilizing MM2. As can be seen, the sn-1 and the sn-2 aliphatic chains can efficiently pack in a mode that is similar, but not identical, to the packing present in the synclinal conformation of the θ_2 torsion angle in phosphatidylcholine (i.e., conformation in panel A). (C) The torsion angle θ_2 in the glycerol backbone in phosphatidylcholine was arranged in a pseudo-antiperiplanar conformation ($\theta_2 = 130°$), and the remaining crystal structure coordinates of phosphatidylethanolamine[30] were utilized as a starting basis set for energy minimization utilizing MM2. As can be seen, the sn-1 aliphatic chain cannot efficiently pack because the trans geometry of the sn-1 carbonyl directs the sn-1 acyl chain nearly perpendicular to the sn-2 aliphatic constituent.

(23) Abraham, R. J.; Gatti, G. *J. Chem. Soc. B* **1969**, 961–968.
(24) Partington, P.; Feeney, J.; Kurgen, A. S. V. *Mol. Pharmacol.* **1972**, *8*, 269–277.
(25) Dodziuk, H.; von Voithenberg, H.; Allinger, N. L. *Tetrahedron* **1982**, *38*, 2811–2819.

ether-linked phospholipids compared to their diacyl phospholipid counterparts.

The differences in the predominant conformational states in each choline glycerophospholipid subclass are further exemplified by analysis of the distribution of conformational states (gauche and antiperiplanar) about the C_3–O_{31} bond (see Figure 1) from the calculated coupling constants of phosphorous and the sn-3 glycerol methylene protons. Although the antiperiplanar conformation is the major conformation in all three choline glycerophospholipid subclasses, differences exist between the relative distribution of gauche and antiperiplanar conformations in each subclass. For example, the fractional percentage of the gauche rotamer in phosphatidylcholine is nearly 50% larger than that present in plasmanylcholine (Table II).

While the distribution of individual conformational states in phospholipids in a micellar aggregation state are likely different from those present in membrane bilayers, the present results clearly indicate that differences in the population distribution of the individual rotamers in each subclass of choline glycerophospholipids are present in at least some organized states. Given the multiplicity of rotameric states in phospholipids (i.e., rotamers of the C_1–C_2 and C_3–O_{31} bonds as well as rotamers of the proximal regions in the aliphatic chains) and the likelihood that specific mosaics of total conformational states selectively and differentially interact with complimentary regions of polypeptides, it is tempting to speculate that alterations in the rotameric distribution of phospholipids in mammalian membranes contribute to the marked subclass selectivity of phospholipases that selectively catalyze hydrolysis of ether-linked phospholipid substrates.[26-29]

Acknowledgment. This research was supported by National Institute of Health Grants HL34839 and HL41250. R.W.G. is the recipient of an Established Investigator award from the American Heart Association.

(26) Wolf, R. A.; Gross, R. W. *J. Biol. Chem.* **1985**, *260*, 7295-7303.
(27) Loeb, L. A.; Gross, R. W. *J. Biol. Chem.* **1986**, *261*, 10467-10470.
(28) Angle, M. J.; Paltauf, F.; Johnston, J. M. *Biochim. Biophys. Acta* **1988**, *962*, 234-240.
(29) Hazen, S. L.; Stuppy, R. J.; Gross, R. W. *J. Biol. Chem.* **1990**, *265*, 10622-10630.
(30) Hitchcock, P. B.; Mason, R.; Thomas, K. M.; Shipley, G. G. *Proc. Natl. Acad. Sci. U.S.A.* **1974**, *71*, 3036-3040.

Experimental and Theoretical Investigation of the Molecular Structure of Cyclopropylgermane

Marwan Dakkouri

Contribution from the Abteilung für Physikalische Chemie, Universität Ulm, 7900 Ulm, Germany. *Received July 23, 1990*

Abstract: In this work the gas-phase molecular structure of cyclopropylgermane (CPG) has been investigated by electron diffraction and ab initio molecular orbital calculations. The geometry optimization has been performed with use of the basis sets 3-21G*, 4-21G*, and STO-3G. The ring parameters (r_a values with 3σ uncertainties) derived from the electron diffraction study are the following: $r(C_1–C_2)$ = 1.521 (7) Å, $r(C_2–C_3)$ = 1.502 (9) Å, r(C–H) = 1.091 (3) Å, and ∠H–C–H = 118.2 (2.3)°. Other parameters are r(Ge–C) = 1.924 (2) Å, ∠C_1–Ge–H_6 = 108.8 (1.2)°, ∠C_1–Ge–ring plane = 55.5 (1.6)°, ∠C_1–H_5–ring plane = 57.3 (1.9)°. Furthermore, both the experimental and the theoretical studies have revealed that the GeH_3 group is tilted toward the ring plane. The values for this tilt angle obtained from electron diffraction and from calculations are 3.4 (2.0)° and 2.1° (when the 4-21G* basis set is used), respectively. This tilt has been rationalized to be the result of hyperconjugative interaction. The geometric parameters of cyclopropylmonofluorogermane, cyclopropyldifluorogermane, and cyclopropyltrifluorogermane also have been optimized. The progressive shortening of the Ge–F bond with increasing fluorination is interpreted as being the consequence of a fluorine negative hyperconjugation effect. The barrier heights for internal rotation for the GeH_3 and SiH_3 groups and their fluorinated counterparts in various compounds have been calculated. Furthermore, the structural results obtained assess the strong π-donor character of the cyclopropyl system and demonstrate that π-acceptor ability of the germyl group is less pronounced than that of the silyl group.

Introduction

Several complementary concepts[1-6] have been evaluated in order to characterize the versatile bonding behavior and the intrinsic nature of electronic interaction between a vast array of charge-withdrawing or -donating substituents and the strained ring fragment as a pseudo-π system.

Until recently only one representative of the series c-Pr-XH_3 (X = group IV element), methylcyclopropane, had been studied. This was the initial reason for synthesizing the cyclopropane series C_3H_5–XY_3 (X = Si, Ge; Y = H, F, Cl)[7,8] and for starting to explore the bonding properties and stabilizing effects of these monosubstituted ring systems by means of electron diffraction[9] and spectroscopic methods.[10,11] The exceptional electronic

(1) Walsh, A. D. *Trans. Faraday Soc.* **1949**, *45*, 179-190.
(2) (a) Hoffmann, R. *Tetrahedron Lett.* **1970**, 2907-2909. (b) Hoffmann, R.; Stohrer, W. D. *J. Am. Chem. Soc.* **1971**, 6941-6948.
(3) Coulson, C. A.; Moffitt, W. E. *Philos. Mag.* **1949**, *40*, 1-35.
(4) (a) Bader, R. F. W.; Nguyen-Dang, T. T.; Tal, Y. *J. Chem. Phys.* **1979**, *70*, 4316-4329. (b) Bader, R. F. W. *Atoms in Molecules, A Quantum Theory*; Clarendon Press: Oxford, 1990.
(5) Politzer, P.; Abrahmsen, L.; Sjoberg, P.; Laurence, P. R. *Chem. Phys. Lett.* **1983**, *102*, 74-78.
(6) Cremer, D.; Gauss, J. *J. Am. Chem. Soc.* **1986**, *108*, 7476-7477.
(7) Dakkouri, M.; Kehrer, H.; Buhmann, P. *Chem. Ber.* **1979**, *112*, 3523-3525.
(8) Dakkouri, M.; Kehrer, H. *Chem. Ber.* **1983**, *116*, 2041-2043.
(9) Dakkouri, M.; Typke, V. *J. Mol. Struct.* **1987**, *158*, 323-337.
(10) (a) Laane, J.; Nour, E. M.; Dakkouri, M. *J. Mol. Spectrosc.* **1983**, *102*, 368-371. (b) Kelly, M. B.; Laane, J.; Dakkouri, M. *J. Mol. Spectrosc.* **1989**, *137*, 82-86. (c) Typke, V.; Botskor, I.; Wiedenmann, K. H. *J. Mol. Spectrosc.* **1986**, *120*, 435-440.
(11) McKean, D. C.; Morrisson, A. R.; Dakkouri, M. *Spectrochim. Acta* **1984**, *A40*, 771-774.

0002-7863/91/1513-7109$02.50/0